FIGURE LEGENDS

FIG. 1

Monocytes contributed to the vulnerability of the PBMCs in patients with diabetes. (*A*)PBMCs were obtained from 33 patients with diabetes and 28 healthy volunteers. Isolated PBMCs were harvested in AIM-V serum-free culture media supplemented with 5 mM glucose for 3 hours and incubated with FITC-labeled anti-CD4, CD14, or CD56 antibodies, together with PE-labeled Annexin-V to assess the frequency of apoptotic cells in each subpopulation of PBMCs. Apoptotic cells were identified by double-staining with PE-labeled Annexin-V and 7-AAD by flow cytometry. The frequencies of apoptotic cells determined as the Annexin-V-positive and 7-AAD-negative population are expressed as mean ± SEM with statistical comparisons for both groups. The non-parametric Mann-Whitney *U* test was used to calculate the *P* value. $*P < 0.05$ $***P < 0.01$ $***P < 0.001$. The PBMCs of patients with diabetes were more susceptible to apoptosis than those of healthy volunteers, and $CD14^+$ monocytes were contributors. (*B*) Among the 33 patients with diabetes, those with poor glycemic control reflected as $HbA_{1c} \geq 9.0$ were more susceptible to apoptosis in $CD14^+$ monocytes. Data are expressed as mean ± SEM with a statistical comparison of both groups. $*P < 0.05$. (*C*) Monocytes were isolated from 15 patients with $HbA_{1c} \geq 9.0$ and 18 patients with $HbA_{1c} < 9.0$. The expression of the BCL-2 gene in their monocytes before and after incubation in AIM-V serum-free media was assessed by RTD-PCR. After 3 h incubation, the expression of BCL-2 was not upregulated in the poor glycemic control group ($HbA_{1c} \geq 9.0$), as compared to the fair control group ($HbA_{1c} < 9.0$). Data are expressed as mean ± SEM with statistical comparisons of both groups. $*P < 0.05$.

FIG. 2

Attenuated phagocytosis activity in diabetic monocytes. Whole PBMCs were incubated with FITC-labeled *E. coli* for 10 minutes followed by PI staining and flow cytometric analysis. (*A*) Gated PI-positive populations were viable leukocyte populations (upper panel). The monocyte population was assessed using granularity (SSC) and size (FSC) (middle panel). For the gated cells indicating viable monocytes, FITC-positive cells were assessed as monocytes containing phagocytosed FITC-labeled *E. coli*. (lower panel). (*B*) The frequency of monocytes containing phagocytosed *E. coli* in patients with diabetes was less than that in healthy volunteers. Data are expressed as means ± SEM. $*P < 0.05$.

FIG. 3

Hyporesponsiveness to TLR ligand stimuli by the monocytes of patients with diabetes. (*A*)-(*D*) Isolated $CD14^+$ monocytes from 33 patients with diabetes and 28 healthy volunteers were cultured in AIM-V serum-free media supplemented with each TLR ligand: PGN, Poly (I:C), and LPS. After 3 h incubation, RNA was isolated from the monocytes and the expression levels of the TNF-α and IL-1β genes were analyzed by RTD-PCR. The basal (pre-stimuli) expression of (*A*) TLR2, TLR3, and TLR4 and (*B*) TNF-α and IL-1β did not differ significantly between the two groups. The TLR ligand-induced expression of (*C*) TNF-α and (*D*) IL-1β was downregulated in the monocytes of patients with diabetes. Data are expressed as means ± SEM. $*P < 0.05$, $**P < 0.01$.

FIG. 4

Monocytes of patients with diabetes were under ER stress. (*A*) The gene expression profiles of representative vulnerable CD14$^+$ monocytes obtained from five patients with diabetes and five healthy volunteers were analyzed using a DNA microarray. Unsupervised hierarchical clustering using 17,184 filtered genes produced two clusters that separated the patients with diabetes from the healthy volunteers without exception. (*B*)–(*C*), The gene expression levels of the ER stress markers, such as CHOP and BiP, on CD14$^+$ monocytes and CD4$^+$ T cells obtained from 33 patients with diabetes and 28 healthy volunteers was analyzed using RTD-PCR. (*B*) The expression levels of CHOP and BiP in monocytes of patients with diabetes were significantly upregulated, as compared to the monocytes of healthy volunteers. Data are expressed as means ± SEM. $*P < 0.05$, $**P < 0.01$. (*C*) The expression levels of CHOP and BiP in T cells of patients with diabetes were similar to those of healthy volunteers. Data are expressed as mean ± SEM. (*D*) Monocytes were obtained from three healthy volunteers and three patients with diabetes (Healthy volunteer 1: 64-year-old man, HbA_{1c} 5.7%; Healthy volunteer 2: 66-year-old man, HbA_{1c} 4.9%; Healthy volunteer 3: 68-year-old woman, HbA_{1c} 5.6%; Diabetic patient 1: 56-year-old man, HbA_{1c} 9.1%; Diabetic patient 2: 64-year-old woman, HbA_{1c} 8.2%; Diabetic patient 3: 71-year-old man, HbA_{1c} 10.2%) and examined them using electron microscopy. In the three patients with diabetes, the concentric, continuous, and regular layer structures of the ER were corrupted, with fewer ribosomes on the ER membrane compared to the ER of the healthy volunteer. ER, endoplasmic reticulum; N, nucleus; M, mitochondrion. Scale bars indicate 100 nm.

FIG. 5

ER stress enhanced the susceptibility of human monocytes to apoptosis. (*A*)–(*B*) Human CD14$^+$ monocytes obtained from a healthy volunteer were incubated in AIM-V culture media supplemented with tunicamycin (1 or 5 μg/ml). The frequency of apoptotic cells was analyzed by flow cytometry every 3 h for 12 h. More apoptotic cells were observed among monocytes treated with tunicamycin for more than 6 h incubation, as compared to untreated monocytes. (*A*) Representative scattergram of Annexin-V and 7-AAD for monocytes treated with tunicamycin. The numbers in each quadrant indicate the percentage of apoptotic cells. (*B*) Apoptotic cells were assessed in triplicate for each condition. Data are expressed as means ± SEM. (*C*) Caspse-3 activity in monocytes treated with tunicamycin increased significantly at 12 h incubation. (*D*) The BCL-2 expression in monocytes incubated with tunicamycin for 12 h was down-regulated. (*E*) The expression levels of the ER stress markers CHOP and BiP in monocytes incubated with tunicamycin for 12 h were significantly up-regulated. Data are expressed as means ± SEM of three independent experiments. Open bars, no treatment; shaded bar, treatment with tunicamycin (1 μg/ml); solid bar, treatment with tunicamycin (5 μg/ml). TM, tunicamycin.

FIG. 6

Expression of pro-inflammatory cytokines in response to TLR ligand stimuli decreased in human monocytes treated with tunicamycin. Isolated human CD14$^+$ monocytes were incubated in AIM-V culture media with tunicamycin (1 or 5 μg/ml) and stimulated using TLR ligands, PGN, and LPS for 6 h. *A–C*, RTD-PCR analysis showed that the expression of TNF-α (*A*), IL-1β (*B*),

and IL-6 (*C*) was down-regulated in human CD14$^+$ monocytes treated with tunicamycin, especially at the higher concentration (5 μg/ml). *D–F*, ELISA showed that the production of TNF-α (*D*), IL-1β (*E*), and IL-6 (*F*) in culture media decreased in human monocytes treated with tunicamycin, especially at the higher concentration (5 μg/ml). Data are expressed as means ± SEM of four independent experiments. Open bars, no treatment; shaded bar, treatment with tunicamycin (1 μg/ml); solid bar, treatment with tunicamycin (5 μg/ml). TM, tunicamycin.

Figure 1

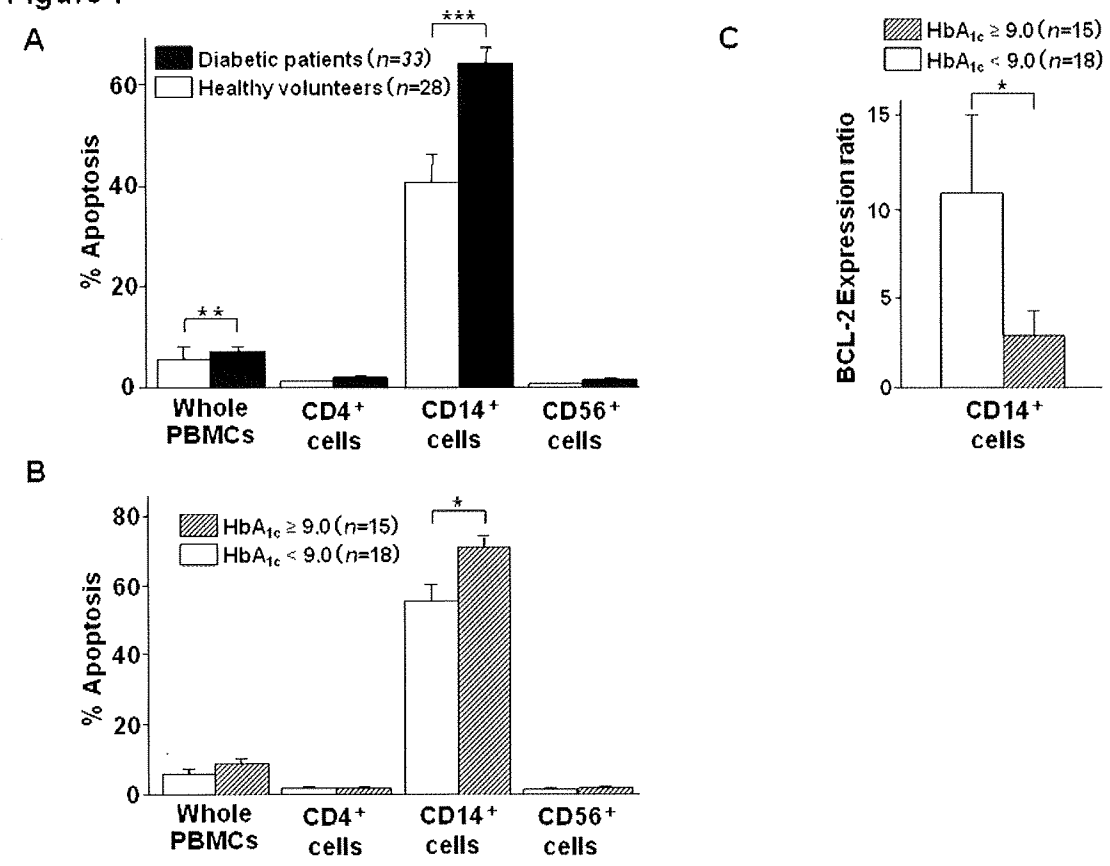

Figure 2

A

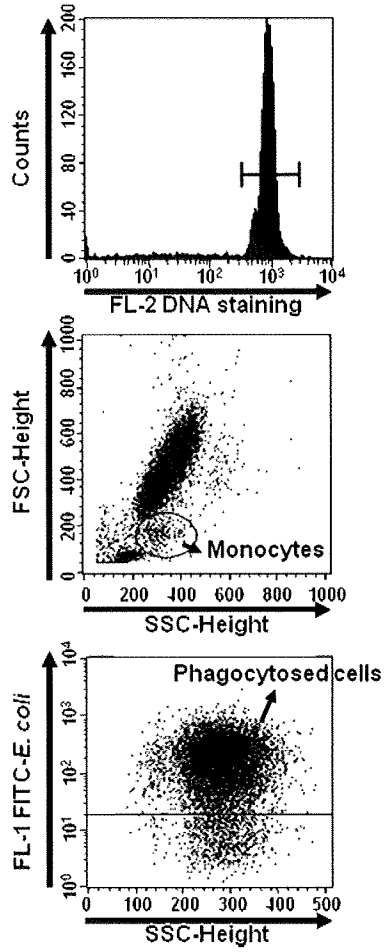
Counts
FL-2 DNA staining
FSC-Height
Monocytes
SSC-Height
FL-1 FITC-E. coli
Phagocytosed cells
SSC-Height

B

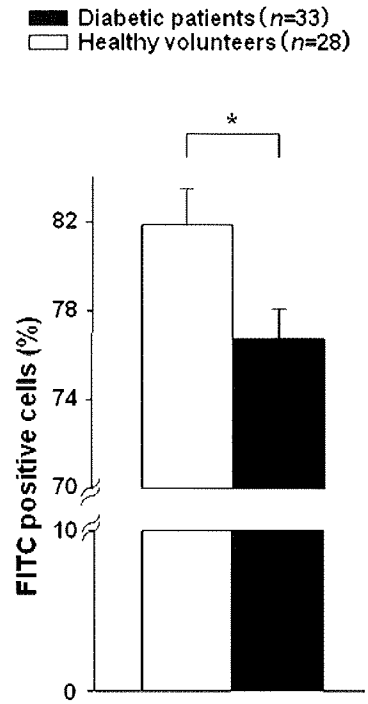
Diabetic patients (n=33)
Healthy volunteers (n=28)
*
FITC positive cells (%)
82
78
74
70
10
0

Figure 3

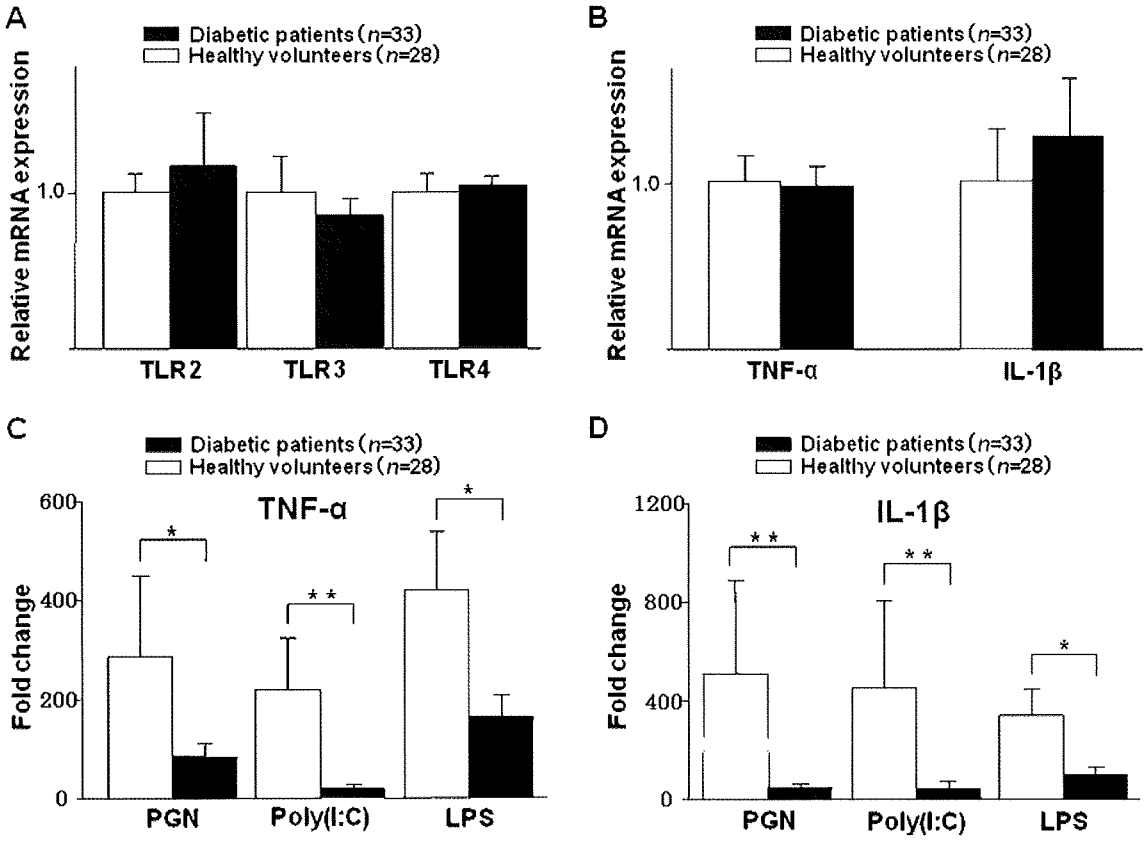
A
Diabetic patients (n=33)
Healthy volunteers (n=28)
Relative mRNA expression
1.0
TLR2
TLR3
TLR4
B
Diabetic patients (n=33)
Healthy volunteers (n=28)
Relative mRNA expression
1.0
TNF-α
IL-1β
C
Diabetic patients (n=33)
Healthy volunteers (n=28)
TNF-α
Fold change
600
400
200
0
*
**
*
PGN
Poly(I:C)
LPS
D
Diabetic patients (n=33)
Healthy volunteers (n=28)
IL-1β
Fold change
1200
800
400
0
**
**
*
PGN
Poly(I:C)
LPS

Figure 4

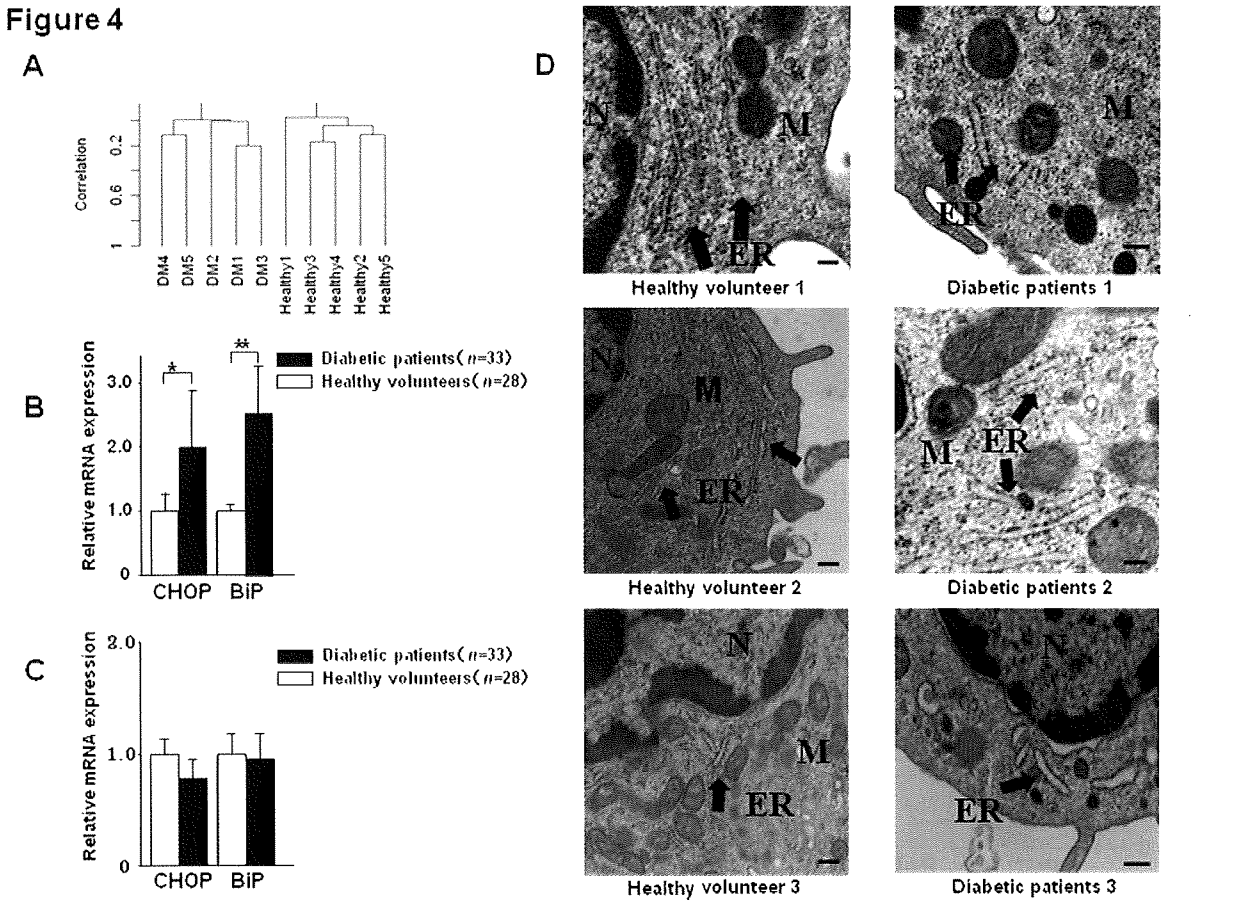
A
Correlation
1
0.6
0.2
DM4
DM5
DM2
DM1
DM3
Healthy1
Healthy3
Healthy4
Healthy2
Healthy5
B
Relative mRNA expression
3.0
2.0
1.0
0
*
**
Diabetic patients(n=33)
Healthy volunteers(n=28)
CHOP
BiP
C
Relative mRNA expression
2.0
1.0
0
Diabetic patients(n=33)
Healthy volunteers(n=28)
CHOP
BiP
D
N
M
ER
Healthy volunteer 1
Diabetic patients 1
Healthy volunteer 2
Diabetic patients 2
Healthy volunteer 3
Diabetic patients 3

Figure 5

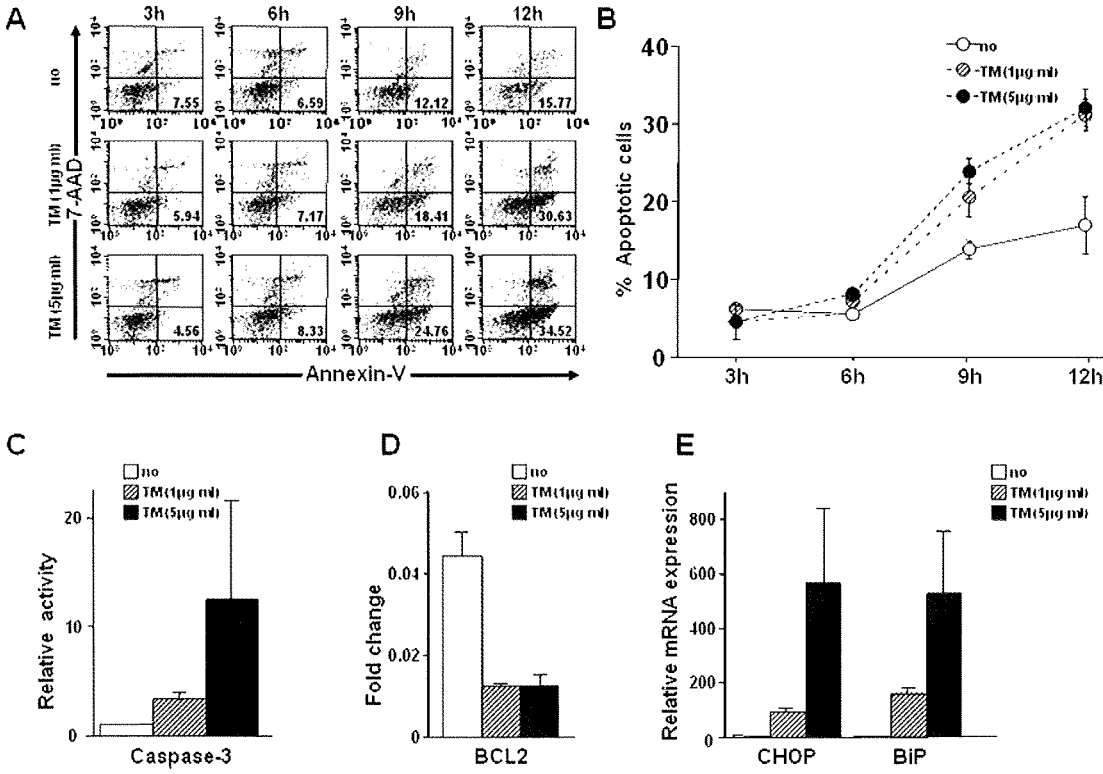
A
3h
6h
9h
12h
no
TM(1μg ml)
TM(5μg ml)
7-AAD
Annexin-V
7.55
6.59
12.12
15.77
5.94
7.17
18.41
30.63
4.56
8.33
24.76
34.52
B
% Apoptotic cells
no
TM(1μg ml)
TM(5μg ml)
C
Relative activity
Caspase-3
D
Fold change
BCL2
E
Relative mRNA expression
CHOP
BiP

Figure 6

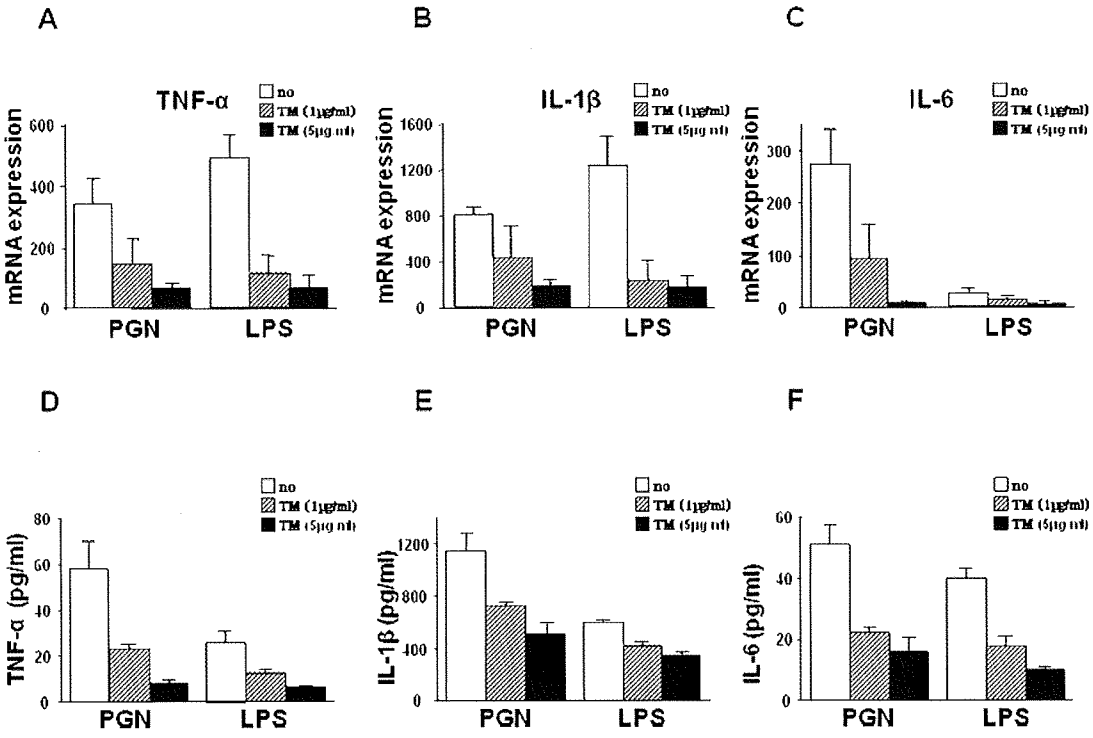
A
B
C
TNF-α
IL-1β
IL-6
no
TM (1μg/ml)
TM (5μg ml)
mRNA expression
PGN
LPS
D
E
F
TNF-α (pg/ml)
IL-1β (pg/ml)
IL-6 (pg/ml)

Supplemental Material can be found at:
http://www.jbc.org/cgi/content/full/M901488200/DC1

⌘ *Author's Choice*

THE JOURNAL OF BIOLOGICAL CHEMISTRY VOL. 284, NO. 22, pp. 14809–14818, May 29, 2009

Palmitate Induces Insulin Resistance in H4IIEC3 Hepatocytes through Reactive Oxygen Species Produced by Mitochondria*[S]

Received for publication, March 5, 2009 Published, JBC Papers in Press, March 30, 2009, DOI 10.1074/jbc.M901488200

Seiji Nakamura[‡], Toshinari Takamura[‡1], Naoto Matsuzawa-Nagata[§], Hiroaki Takayama[‡], Hirofumi Misu[‡], Hiroyo Noda[‡], Satoko Nabemoto[‡], Seiichiro Kurita[‡], Tsuguhito Ota[‡], Hitoshi Ando[‡], Ken-ichi Miyamoto[§], and Shuichi Kaneko[‡]

From the [‡]Department of Disease Control and Homeostasis, Kanazawa University Graduate School of Medical Science, and the [§]Department of Medicinal Informatics, Kanazawa University Hospital, 13-1 Takara-machi, Kanazawa 920-8641, Japan

Visceral adiposity in obesity causes excessive free fatty acid (FFA) flux into the liver via the portal vein and may cause fatty liver disease and hepatic insulin resistance. However, because animal models of insulin resistance induced by lipid infusion or a high fat diet are complex and may be accompanied by alterations not restricted to the liver, it is difficult to determine the contribution of FFAs to hepatic insulin resistance. Therefore, we treated H4IIEC3 cells, a rat hepatocyte cell line, with a monounsaturated fatty acid (oleate) and a saturated fatty acid (palmitate) to investigate the direct and initial effects of FFAs on hepatocytes. We show that palmitate, but not oleate, inhibited insulin-stimulated tyrosine phosphorylation of insulin receptor substrate 2 and serine phosphorylation of Akt, through c-Jun NH_2-terminal kinase (JNK) activation. Among the well established stimuli for JNK activation, reactive oxygen species (ROS) played a causal role in palmitate-induced JNK activation. In addition, etomoxir, an inhibitor of carnitine palmitoyltransferase-1, which is the rate-limiting enzyme in mitochondrial fatty acid β-oxidation, as well as inhibitors of the mitochondrial respiratory chain complex (thenoyltrifluoroacetone and carbonyl cyanide *m*-chlorophenylhydrazone) decreased palmitate-induced ROS production. Together, our findings in hepatocytes indicate that palmitate inhibited insulin signal transduction through JNK activation and that accelerated β-oxidation of palmitate caused excess electron flux in the mitochondrial respiratory chain, resulting in increased ROS generation. Thus, mitochondria-derived ROS induced by palmitate may be major contributors to JNK activation and cellular insulin resistance.

Insulin is the major hormone that inhibits gluconeogenesis in the liver. Visceral adiposity in obesity causes hepatic steatosis and insulin resistance. In an insulin-resistant state, impaired insulin action allows enhancement of glucose production in the liver, resulting in systemic hyperglycemia (1) and contributing to the development of type 2 diabetes. In addition, we have demonstrated experimentally that insulin resistance accelerated the pathology of steatohepatitis in genetically obese diabetic OLETF rats (2). In contrast, lipid-induced oxidative stress caused steatohepatitis and hepatic insulin resistance in mice (3). In fact, steatosis of the liver is an independent predictor of insulin resistance in patients with nonalcoholic fatty liver disease (4).

It remains unclear whether hepatic steatosis causally contributes to insulin resistance or whether it is merely a resulting pathology. Excessive dietary free fatty acid (FFA)[2] flux into the liver via the portal vein may cause fatty liver disease and hepatic insulin resistance. Indeed, elevated plasma FFA concentrations correlate with obesity and decreased target tissue insulin sensitivity (5).

Experimentally, lipid infusion or a high fat diet that increases circulating FFA levels promotes insulin resistance in the liver. Candidate events linking FFA to insulin resistance *in vivo* are the up-regulation of SREBP-1c (6), inflammation caused by activation of c-Jun amino-terminal kinase (JNK) (7) or IKKβ (8), endoplasmic reticulum (ER) stress (9), ceramide (10, 11), and TRB3 (12).

However, which event is the direct and initial target of FFA in the liver is unclear. Insulin resistance induced by lipid infusion or a high fat diet is complex and may be accompanied by alterations not restricted to the liver, making it difficult to determine the contribution of FFAs to hepatic insulin resistance. For example, hyperinsulinemia and hyperglycemia secondary to the initial event also may contribute to the development of diet-induced insulin resistance *in vivo* (6).

To address the early event(s) triggering the development of high fat diet- or obesity-induced insulin resistance, we investigated the molecular mechanism(s) underlying the direct action of FFA on hepatocytes to cause insulin resistance *in vitro*, using the rat hepatocyte cell line H4IIEC3. We found that mitochondria-derived reactive oxygen species (ROS) were a cause of palmitate-induced insulin resistance in hepatocytes.

* This work was supported by grants-in-aid from the Ministry of Education, Culture, Sports, Science, and Technology of Japan.
⌘ *Author's Choice*—Final version full access.
[S] The on-line version of this article (available at http://www.jbc.org) contains supplemental Figs. 1–8.
[1] To whom correspondence should be addressed. Tel.: 81-76-265-2233; Fax: 81-76-234-4250; E-mail: ttakamura@m-kanazawa.jp.

[2] The abbreviations used are: FFA, free fatty acid; IRS, insulin receptor substrate; JNK, c-Jun NH_2-terminal kinase; ER, endoplasmic reticulum; ROS, reactive oxygen species; NAC, *N*-acetyl-L-cysteine; H2DCFDA, 2′,7′-dichlorofluorescin diacetate; OXPHOS, oxidative phosphorylation; PVDF, polyvinylidene difluoride.

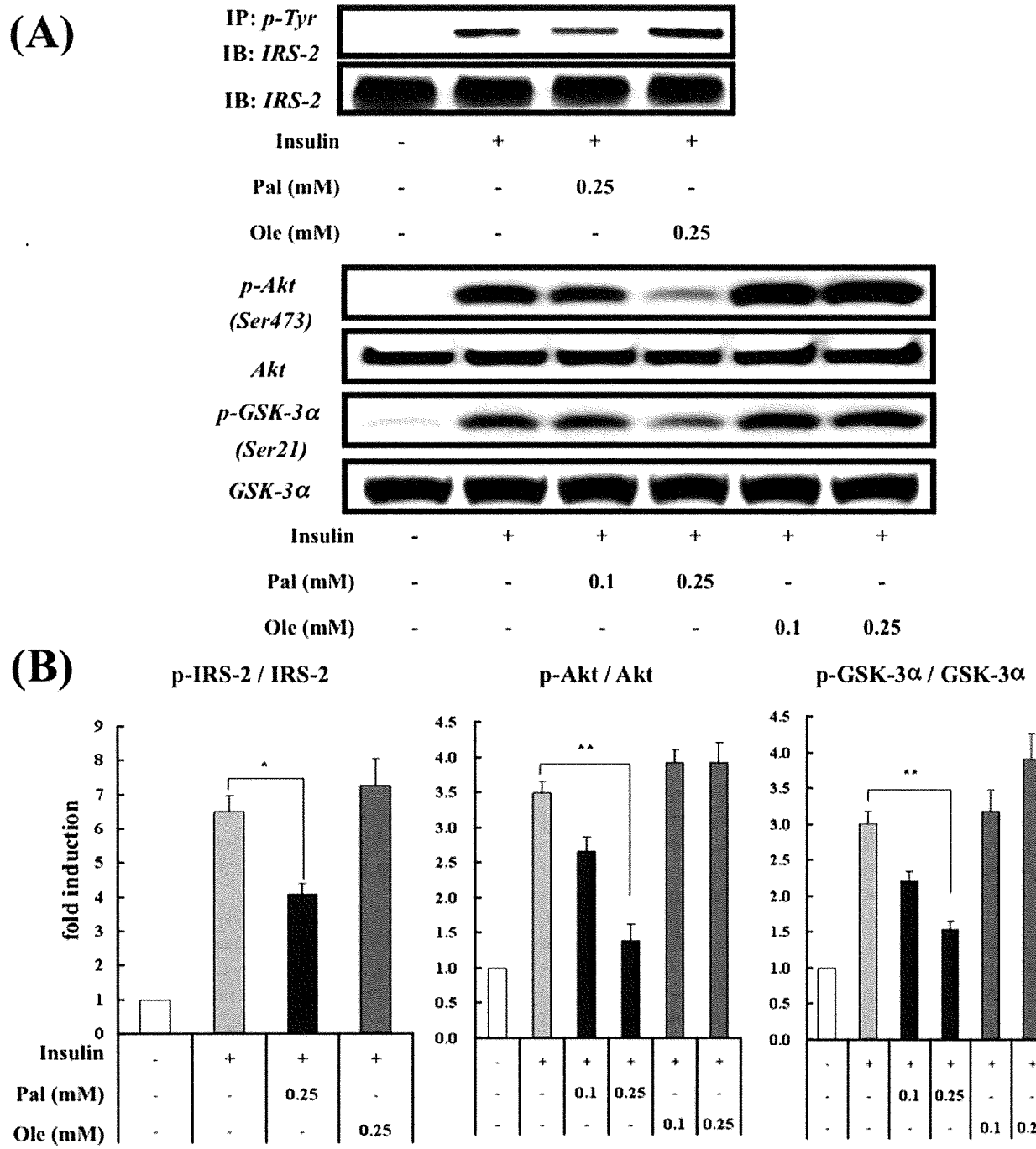

FIGURE 1. **Effects of palmitate and oleate on insulin-stimulated tyrosine phosphorylation of IRS-2 and serine phosphorylation of Akt and GSK-3 in H4IIEC3 hepatocytes.** *A*, H4IIEC3 cells were incubated in the presence or absence of palmitate (*Pal*) or oleate (*Ole*) for 16 h prior to stimulation with insulin (1 ng/ml, 15 min). Total cell lysates were resolved by SDS-PAGE, transferred to a PVDF membrane, and immunoblotted (*IB*) with the indicated antibodies. Total cell lysates were subjected to immunoprecipitation (*IP*) with phosphotyrosine antibody prior to SDS-PAGE to examine tyrosine phosphorylation of IRS-2. Detection was by enhanced chemiluminescence. Representative blots are shown. *B*, the values from densitometry of three (p-IRS-2), eight (p-Akt), or five (p-GSK-3α) independent experiments were normalized to the level of total IRS-2, Akt, or GSK-3α protein, respectively, and expressed as the mean -fold increase over control ± S.E. *, $p < 0.05$ *versus* insulin treatment alone. **, $p < 0.01$ *versus* insulin treatment alone.

EXPERIMENTAL PROCEDURES

Materials—The antibody against IRS-2 was purchased from Upstate Biotechnology, Inc. (Lake Placid, NY). Antibodies against phosphotyrosine, Akt, phospho-Akt (Ser^{473}), stress-activated protein kinase/JNK, phospho-stress-activated protein kinase/JNK (Thr^{183}/Tyr^{185}), and phospho-GSK (glycogen synthase kinase)-3 ($Ser^{21/9}$) were purchased from Cell Signaling Technology (Beverly, MA). Antibodies against GSK-3 and phospho-c-Jun were from Santa Cruz Biotechnology, Inc. (Santa Cruz, CA). Insulin from porcine pancreas, sodium

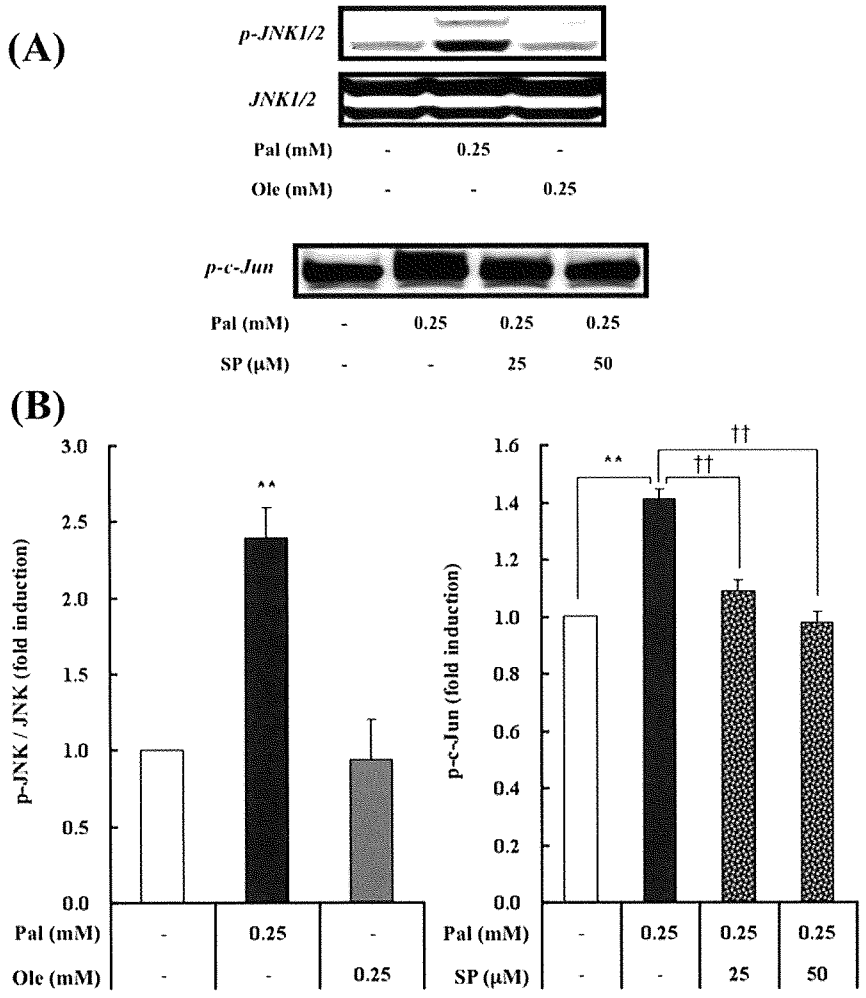

FIGURE 2. **Effects of palmitate and oleate on JNK activation in H4IIEC3 hepatocytes.** *A*, H4IIEC3 cells were incubated in the presence or absence of FFAs (palmitate (*Pal*) or oleate (*Ole*)) and the JNK inhibitor SP600125 (*SP*) for 16 h. Total cell lysates were resolved by SDS-PAGE, transferred to a PVDF membrane, and immunoblotted with the indicated antibodies. Detection was by enhanced chemiluminescence. Representative blots are shown. *B*, the values from densitometry of four (p-JNK) independent experiments were normalized to the level of total JNK (p-c-Jun was not normalized; $n = 4$) and expressed as the mean -fold increase over control ± S.E. **, $p < 0.01$ *versus* control. ††, $p < 0.01$ *versus* palmitate treatment.

palmitate, sodium oleate, myriocin, *N*-acetyl-L-cysteine, rotenone, thenoyltrifluoroacetone, cyanide *m*-chlorophenylhydrazone, oxypurinol, etomoxir, and tunicamycin was obtained from Sigma. SP600125 and apocynin were from Calbiochem. DL-α-tocopherol and 2′,7′-dichlorofluorescin diacetate (H_2DCFDA) were from Wako (Osaka, Japan).

Cell Culture and Fatty Acid Treatment—Studies were performed in the rat hepatoma cell line H4IIEC3, purchased from the American Type Culture Collection (Manassas, VA). Cells were cultured in Dulbecco's modified Eagle's medium (Invitrogen) supplemented with 10% fetal bovine serum (Invitrogen), penicillin (100 units/ml), and streptomycin (0.1 mg/ml; Invitrogen). The cells were cultured at 37 °C in a humidified atmosphere containing 5% CO_2, with medium changes three times a week. All studies were conducted using 80–90% confluent cells, which were treated with the indicated concentrations of FFAs in the presence of 2% FFA-free bovine serum albumin (Sigma).

Cell Harvest and Western Blot Analysis—H4IIEC3 hepatocytes, grown to 80–90% confluence in 6-well plates, were treated with the indicated reagents for 16 h in Dulbecco's modified Eagle's medium. After treatment, the cells were stimulated with insulin (1 ng/ml) for 15 min. Then the cells were washed with ice-cold phosphate-buffered saline and lysed in buffer containing 20 mM Tris-HCl (pH 7.5), 5 mM EDTA, 1% Nonidet P-40, 2 mM Na_3VO_4, 100 mM NaF, and a protease inhibitor mixture (Sigma). After sonication with a Bioruptor (Cosmo Bio, Tokyo, Japan), the lysates were centrifuged to remove insoluble materials. The supernatants (10 μg/lane) were separated by SDS-PAGE and transferred onto polyvinylidene difluoride membranes (Millipore, Billerica, MA). For detection of phosphotyrosine insulin receptor and phosphotyrosine IRS-2, the supernatants (400 μg of protein) were immunoprecipitated with a phosphotyrosine antibody and protein G beads for 2 h at 4 °C before SDS-PAGE. The membranes were blocked in a buffer containing 5% nonfat milk, 50 mM Tris (pH 7.6), 150 mM NaCl, and 0.1% Tween 20 (TBS-T) for 1 h at room temperature. They were then incubated with specific primary antibodies and subsequently with horseradish peroxidase-linked secondary antibodies. Signals were detected with a chemiluminescence detection system (ECL Plus Western blotting detection reagents; GE Healthcare). Densitometric analysis was conducted directly on the blotted membrane, using a CCD camera system (LAS-3000 Mini; Fujifilm, Tokyo, Japan) and Scion Image software.

Quantitative Real Time PCR—Total RNA was extracted from cultured H4IIEC3 hepatocytes using an RNeasy mini kit (Qiagen, Germantown, MD), according to the manufacturer's protocol. The cDNA was synthesized from total RNA (100 ng) using random hexamer primers, N_6, and a high capacity cDNA reverse transcription kit (Applied Biosystems, Foster City, CA). Quantitative real time PCR was performed with an ABI Prism 7900HT (Applied Biosystems). The set of specific primers and TaqMan probes in the present study was obtained from Applied Biosystems. The PCR conditions were one cycle at 50 °C for 2 min and 95 °C for 10 min, followed by 40 cycles at 95 °C for 15 s and 60 °C for 1 min.

Analysis of XBP-1 (X-box-binding Protein-1) mRNA Splicing—Total RNA was extracted from H4IIEC3 hepatocytes, and

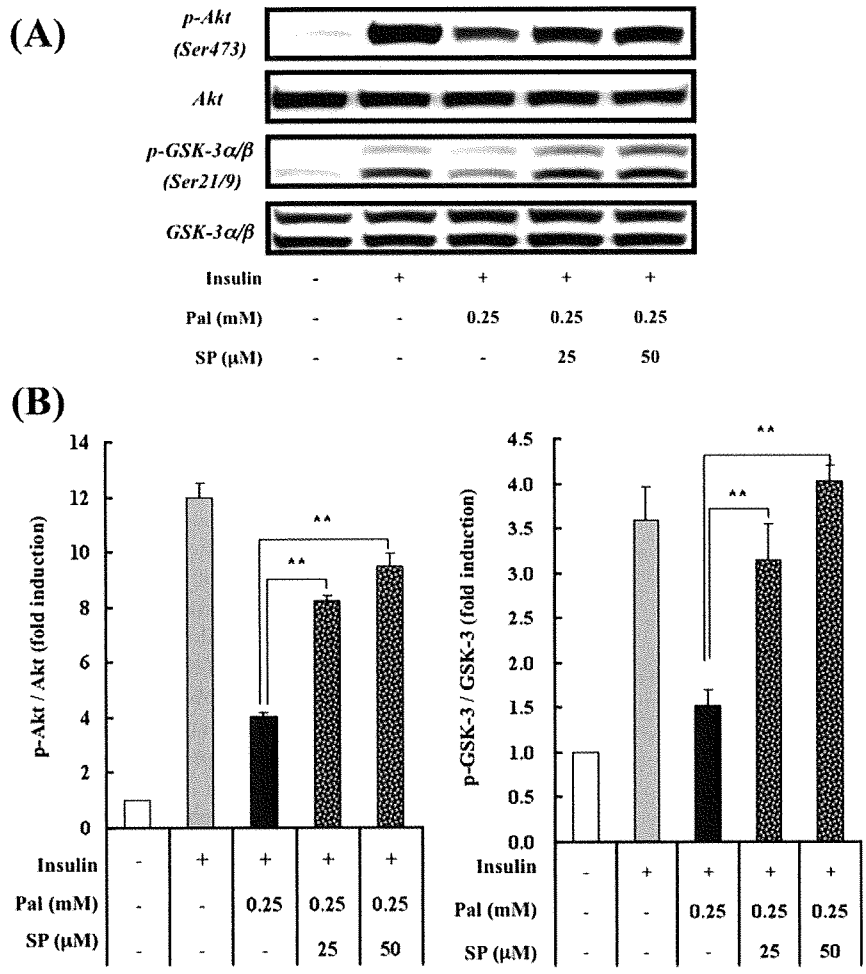

FIGURE 3. **Effect of a JNK inhibitor on palmitate-induced alterations in insulin-stimulated phosphorylation of Akt and GSK-3 in H4IIEC3 hepatocytes.** *A*, H4IIEC3 cells were incubated in the presence or absence of palmitate (*Pal*) and the JNK inhibitor SP600125 (*SP*) for 16 h prior to stimulation with insulin (1 ng/ml, 15 min). Total cell lysates were resolved by SDS-PAGE, transferred to a PVDF membrane, and immunoblotted with the indicated antibodies. Detection was enhanced by chemiluminescence. Representative blots are shown. *B*, the values from densitometry of four (p-Akt or p-GSK-3) independent experiments were normalized to the level of total Akt or GSK-3 protein, respectively, and expressed as the mean -fold increase over control ± S.E. **, $p < 0.01$ *versus* palmitate treatment.

cDNA was synthesized as described above. The cDNA was amplified with a pair of primers (reverse 5′-CCA TGG GAA GAT GTT CTG GG-3′ and forward 5′-ACA CGC TTG GGG ATG AAT GC-3′) corresponding to the rat XBP-1 cDNA. The PCR conditions were initial denaturation at 94 °C for 3 min, followed by 30 cycles of amplification (94 °C for 30 s, 58 °C for 30 s, 72 °C for 30 s) and a final extension at 72 °C for 3 min. The PCR products were separated by 2.5% agarose gel electrophoresis.

Measurement of Intracellular ROS—The intracellular formation of ROS was detected using the fluorescent probe H_2DCFDA, according to a published method (13). Briefly, H4IIEC3 hepatocytes, grown to 70–80% confluence in 96-well plates, were treated with the indicated reagents in Dulbecco's modified Eagle's medium for 8 h. After treatment, the cells were washed with phosphate-buffered saline, loaded with 10 μM H_2DCFDA, and incubated for 30 min at 37 °C. The fluorescence was analyzed using a plate reader (Fluoroskan Ascent FL, ThermoLab Systems, Franklin, MA).

Measurement of Protein Carbonyls—The cellular concentration of proteins containing carbonyl groups (those that react with 2,4-dinitrophenylhydrazine to form the corresponding hydrazone) was determined spectrophotometrically using a protein carbonyl assay kit (Cayman Chemical, Ann Arbor, MI) according to the manufacturer's instructions and as described previously (14).

Statistical Analysis—All values are given as means ± S.E. Differences between two groups were assessed using unpaired, two-tailed *t* tests. Data involving more than two groups were assessed by one-way analysis of variance. All calculations were performed with SPSS (version 12.0 for Windows; SPSS, Chicago, IL).

RESULTS

Palmitate Inhibited Insulin Receptor-mediated Signaling—Two long chain fatty acids were chosen for the study: palmitate, a C16:0 saturated fatty acid, and oleate, a C18:1 monounsaturated fatty acid. To examine whether FFAs impaired insulin signal transduction in H4IIEC3 hepatocytes, we assessed the effect of FFAs on insulin-stimulated tyrosine phosphorylation of IRS-2 and serine phosphorylation of Akt and GSK-3α (Fig. 1). Incubation with 0.25 mM palmitate inhibited insulin-stimulated tyrosine phosphorylation of IRS-2 by 40% in H4IIEC3 cells. Downstream of IRS-2, insulin-stimulated serine phosphorylation of Akt and GSK-3α were also inhibited by 0.25 mM palmitate treatment, by 80 and 70%, respectively, indicating an insulin-resistant state. However, the protein levels of total IRS-2, Akt, and GSK-3 were unaffected by palmitate. Furthermore, we confirmed that palmitate, but not oleate, impaired insulin-stimulated Akt serine phosphorylation in the human hepatoma cell line HepG2 (supplemental Fig. 1).

JNK Activation by Palmitate Contributes to Palmitate-induced Insulin Resistance—JNK, a stress-activated protein kinase, has been reported to phosphorylate IRS-1 and -2 at serine residues (15, 16). Serine phosphorylation of IRSs impairs IRS tyrosine phosphorylation, leading to a reduction in insulin receptor-mediated signaling. Many studies have verified the role of JNK in fat-induced insulin resistance in several experimental systems (7, 17, 18). Thus, we next examined the effect of FFAs on JNK activation and its involvement in insulin signaling. Palmitate, but not oleate, dramatically increased phosphoryla-

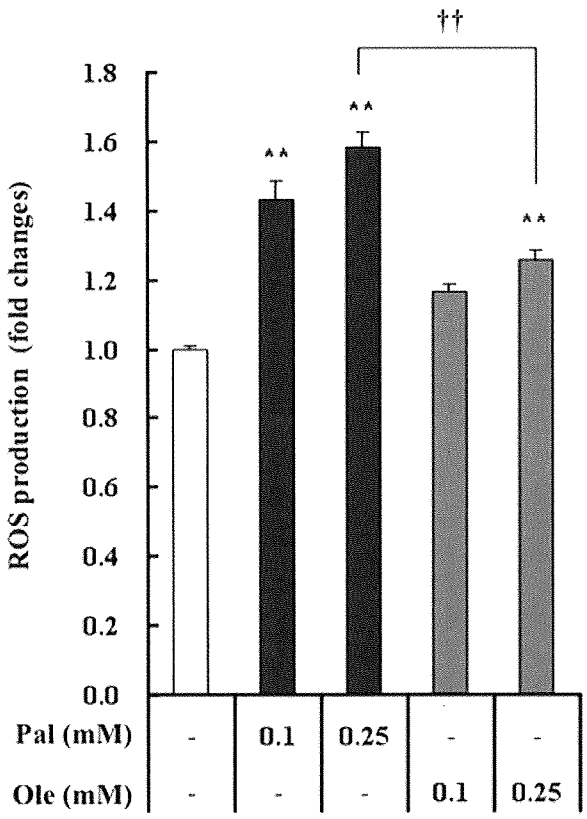

FIGURE 4. **Effect of palmitate on oxidative stress in H4IIEC3 hepatocytes.** H4IIEC3 cells were incubated in the presence or absence of palmitate (*Pal*) or oleate (*Ole*) for 8 h. Intracellular ROS production was quantified using the fluorescent probe H_2DCFDA. The values are expressed as mean -fold increase over control ± S.E. ($n = 4$). **, $p < 0.01$ *versus* control. ††, $p < 0.01$ *versus* 0.25 mM palmitate treatment.

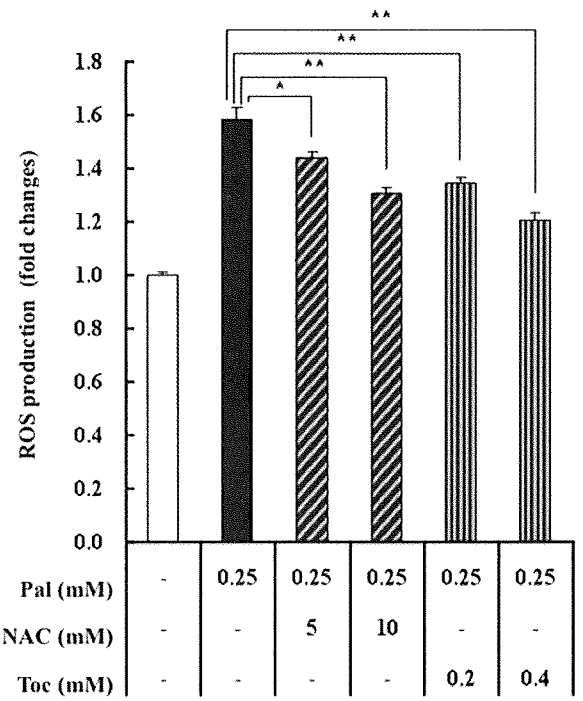

FIGURE 5. **Effects of antioxidants on palmitate-induced intracellular ROS production in H4IIEC3 hepatocytes.** H4IIEC3 cells were incubated in the presence or absence of palmitate (*Pal*) and antioxidants for 8 h. Intracellular ROS production was quantified using the fluorescent probe H_2DCFDA. The values are expressed as mean -fold increase over control ± S.E. ($n = 4$). *, $p < 0.05$ *versus* palmitate treatment alone. **, $p < 0.01$ *versus* palmitate treatment alone. *NAC*, *N*-acetyl-L-cysteine; *Toc*, α-tocopherol.

ted JNK and c-Jun (Fig. 2). A potent and selective inhibitor of JNK, SP600125 (19), reversed the palmitate-induced phosphorylation of c-Jun (Fig. 2), suggesting that palmitate activated JNK. To test whether palmitate-induced JNK activation mediated cellular insulin resistance, we inhibited the JNK pathway with SP600125. SP600125 dose-dependently improved insulin-stimulated serine phosphorylation of Akt and GSK-3 in H4IIEC3 hepatocytes exposed to palmitate (Fig. 3). These results suggest that JNK activation by palmitate contributed to palmitate-induced insulin resistance.

Pathways for SREBP-1c and ER Stress Are Not Involved in Palmitate-induced JNK Activation and Insulin Resistance in H4IIEC3 Hepatocytes—The SREBP-1c pathway has been reported to play a role in diet-induced insulin resistance *in vivo*. Ide *et al.* (6) found that high sucrose diet-induced hyperglycemia and hyperinsulinemia up-regulated hepatic expression of SREBP-1c, leading to down-regulation of IRS-2 at the transcriptional level. However, in the present study, palmitate dramatically down-regulated the expression of SREBP-1c in H4IIEC3 hepatocytes (supplemental Fig. 2). Consistent with this, the mRNA (supplemental Fig. 2) and protein (Fig. 1) levels of IRS-2 were unaffected by palmitate. Thus, palmitate itself did not appear to cause insulin resistance in hepatocytes via the SREBP-1c pathway.

ER stress is induced in insulin-resistant states, such as obesity and type 2 diabetes, and in turn, this stress has been shown to lead to the inhibition of insulin signaling, through overactivation of JNK (9). Since excessive FFAs have been shown to trigger ER stress in pancreatic β-cells (20), we examined whether palmitate caused ER stress in H4IIEC3 hepatocytes. ER stress induces the spliced form of XBP-1 (XBP-1s), which up-regulates the transcription of molecular chaperones, including GRP78 (78-kDa glucose-regulated/binding immunoglobulin protein) (21). Palmitate at 0.25 mM did not alter the expression level of GRP78 mRNA or the splicing pattern of XBP-1, unlike tunicamycin, an agent commonly used to induce ER stress (supplemental Fig. 3). Next, we compared the impact of palmitate and tunicamycin on insulin-stimulated signal transduction and JNK activation (supplemental Fig. 4). The inhibitory effect of tunicamycin on insulin-stimulated serine phosphorylation of Akt was mild and not significant compared with that of palmitate. Additionally, the increment in phosphorylated JNK by tunicamycin was lower and not significant compared with that of palmitate. These results suggest that ER stress played a minor role in palmitate-induced JNK activation and cellular insulin resistance in H4IIEC3 hepatocytes.

Palmitate Induces ROS Production—In addition to ER stress, increased cellular ROS levels are known to stimulate threonine phosphorylation of JNK (22). Indeed, ROS levels are increased in clinical conditions associated with insulin resistance, such as sepsis, burn injuries, obesity, and type 2 diabetes (23). Furthermore, FFAs have been reported to generate ROS in various

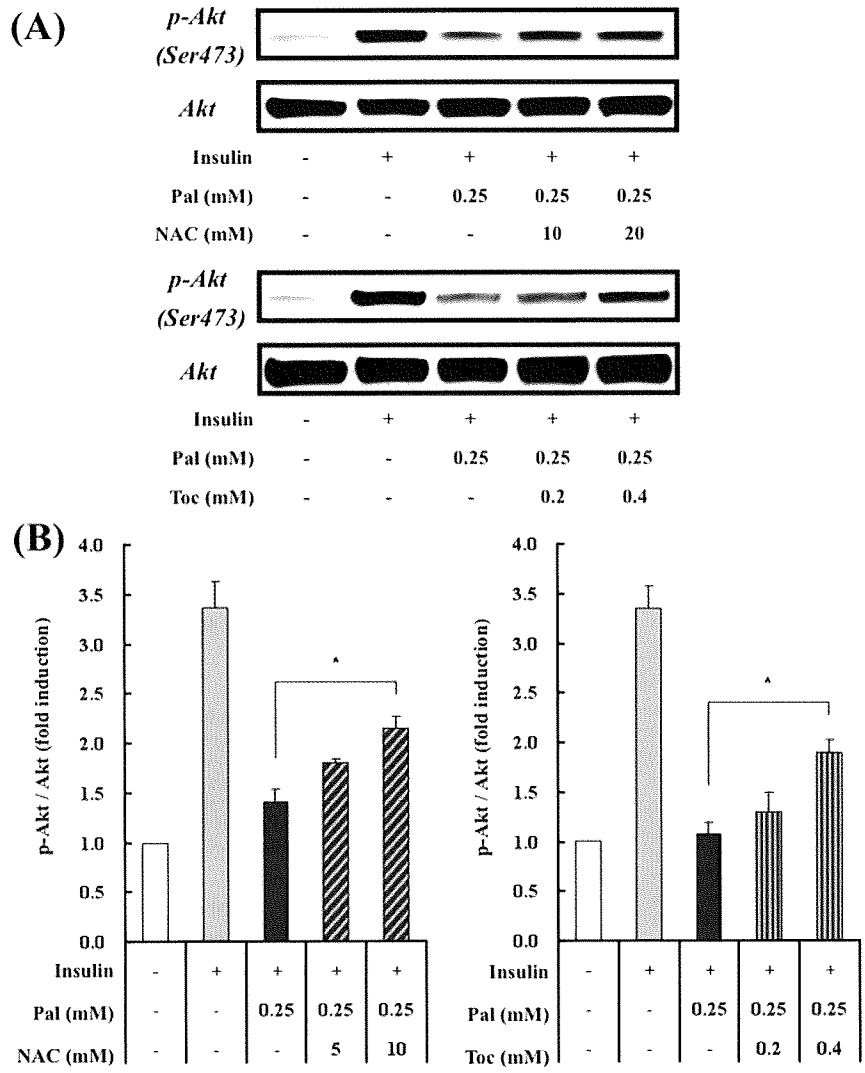

FIGURE 6. **Effects of antioxidants on palmitate-induced alterations in insulin-stimulated serine phosphorylation of Akt in H4IIEC3 hepatocytes.** *A*, H4IIEC3 cells were incubated in the presence or absence of palmitate (*Pal*) and antioxidants for 16 h prior to stimulation with insulin (1 ng/ml, 15 min). Total cell lysates were resolved by SDS-PAGE, transferred to a PVDF membrane, and immunoblotted with the indicated antibodies. Detection was by enhanced chemiluminescence. Representative blots are shown. *B*, the values from densitometry of four (NAC) or five (α-tocopherol) independent experiments were normalized to the level of total Akt protein and expressed as the mean -fold increase over control ± S.E. *, $p < 0.05$ *versus* palmitate treatment. *NAC*, *N*-acetyl-L-cysteine; *Toc*, α-tocopherol.

cells, such as pancreatic islet cells (24), cardiac myocytes (25), and adipocytes (23).

Thus, we hypothesized that palmitate increased intracellular ROS production and thereby activated JNK, leading to the impaired insulin signaling. To evaluate this, H4IIEC3 hepatocytes were incubated with H_2DCFDA, a fluorescent probe, to visualize intracellular ROS, with or without palmitate. H_2DCFDA-associated fluorescence was elevated by 58% after incubation with 0.25 mM palmitate for 8 h, and palmitate induced more ROS production than oleate (Fig. 4). Consistent with this, the amount of protein carbonyls, a marker of oxidative stress, significantly increased in palmitate-treated hepatocytes (4.6 ± 0.5 nmol/mg protein), compared with control cells (3.1 ± 0.4 nmol/mg protein). These results suggest that FFAs, especially palmitate, can cause ROS production and oxidative stress in H4IIEC3 hepatocytes.

Antioxidants Prevent Palmitate-induced Insulin Resistance—We next sought to test whether palmitate-induced ROS overproduction had a causal role in insulin resistance by assessing whether two antioxidant reagents, *N*-acetyl-L-cysteine (NAC) and α-tocopherol, could also act as insulin sensitizers. NAC and α-tocopherol dose-dependently suppressed palmitate-induced intracellular ROS production; NAC at 10 mM and α-tocopherol at 0.4 mM suppressed ROS production by 50 and 60%, respectively (Fig. 5). In parallel with decreased ROS levels, the antioxidants recovered the insulin-stimulated Akt phosphorylation impaired by palmitate; NAC at 10 mM and α-tocopherol at 0.4 mM recovered the phosphorylation by 40 and 35%, respectively (Fig. 6). Furthermore, these antioxidants suppressed palmitate-induced JNK phosphorylation; NAC at 10 mM and α-tocopherol at 0.4 mM suppressed it by 80 and 55%, respectively (Fig. 7). These results suggest that palmitate increased ROS levels in H4IIEC3 hepatocytes and thereby activated JNK, resulting in insulin resistance.

Palmitate Induces ROS Overproduction in Mitochondria—To define the source of ROS induced by palmitate in H4IIEC3 hepatocytes, we examined the cellular pathway involved in ROS production, including NADPH oxidase, xanthine oxidase, and mitochondria-mediated pathways. Palmitate-induced ROS production was markedly suppressed by rotenone, an inhibitor of mitochondrial respiratory chain complex I; thenoyltrifluoroacetone, an inhibitor of mitochondrial respiratory chain complex II; and carbonyl cyanide *m*-chlorophenylhydrazone, an uncoupler of oxidative phosphorylation (Fig. 8). In contrast, ROS production in palmitate-treated H4IIEC3 cells was not suppressed by apocynin, an inhibitor of NADPH oxidase, or oxypurinol, an inhibitor of xanthine oxidase. These results suggest that the mitochondrial respiratory chain is involved in palmitate-induced ROS overproduction in H4IIEC3 hepatocytes.

Palmitate Increases ROS through the Mitochondrial Fatty Acid β-Oxidation Respiratory Chain—FFAs are metabolized in the mitochondrial fatty acid β-oxidation pathway, which sup-

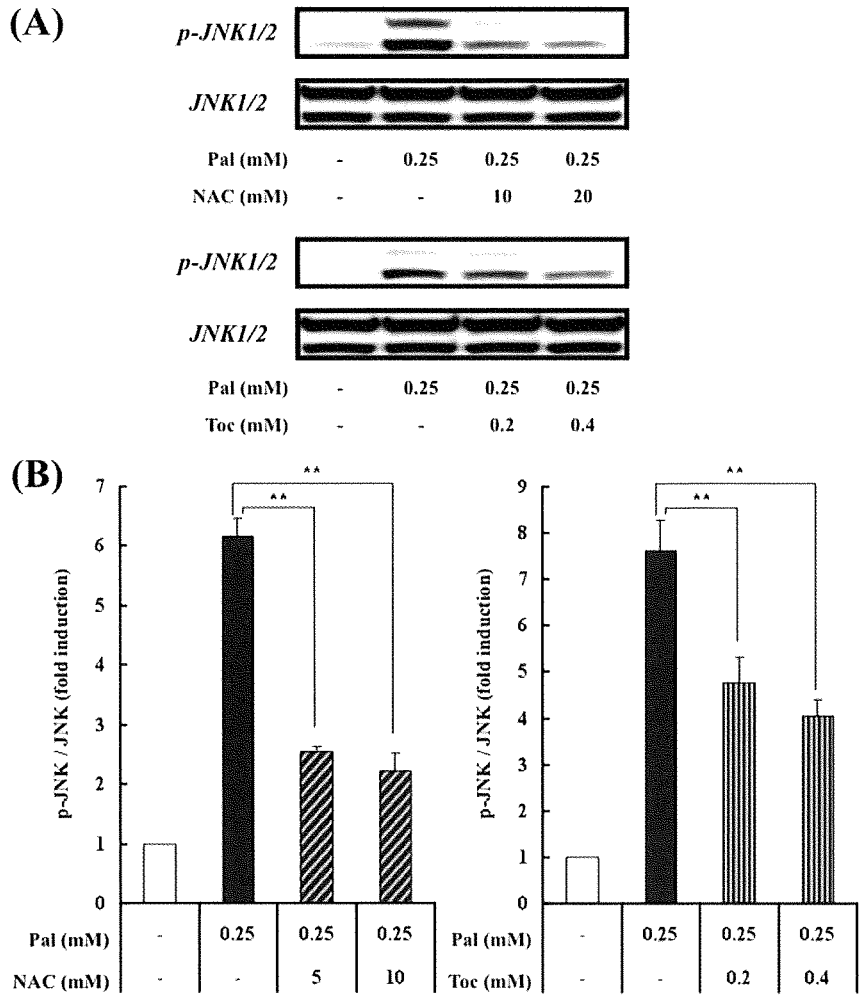

FIGURE 7. **Effects of antioxidants on palmitate-induced JNK activation in H4IIEC3 hepatocytes.** *A*, H4IIEC3 cells were incubated in the presence or absence of palmitate (*Pal*) and antioxidants for 16 h. Total cell lysates were resolved by SDS-PAGE, transferred to a PVDF membrane, and immunoblotted with the indicated antibodies. Detection was by enhanced chemiluminescence. Representative blots are shown. *B*, the values from densitometry of four (NAC or α-tocopherol) independent experiments were normalized to the level of total JNK protein and expressed as the mean -fold increase over control ± S.E. **, $p < 0.01$ *versus* palmitate treatment alone. *Toc*, α-tocopherol.

plies the mitochondrial respiratory chain with electrons. Large amounts of electrons entering the respiratory chain may cause abnormal reduction of oxygen, leading to ROS production. Thus, we next examined whether palmitate-induced ROS production was dependent on mitochondrial fatty acid β-oxidation. CPT-1a (carnitine palmitoyltransferase-1a) is the rate-limiting enzyme in mitochondrial fatty acid β-oxidation. As expected, etomoxir, a CPT-1 inhibitor, decreased palmitate-induced ROS production, by 80% (Fig. 9*A*). Furthermore, palmitate, but not oleate, significantly increased expression of the *CPT-1a* gene (Fig. 9*B*). This up-regulation may contribute to palmitate-induced ROS overproduction, because the accelerated β-oxidation should cause excessive electron flux in the respiratory chain.

DISCUSSION

In the present study, we investigated the direct action of fatty acids on insulin signaling in hepatocytes. The saturated fatty acid palmitate, but not the unsaturated fatty acid oleate, impaired insulin-induced tyrosine phosphorylation of IRS-2, serine phosphorylation of Akt, and serine phosphorylation of GSK-3α, all of which are indicative of insulin resistance in cultured H4IIEC3 hepatocytes (Fig. 10). Unlike *in vivo* findings (6), the expression of the *SREBP-1c* gene was down-regulated by adding palmitate to cultured H4IIEC3 hepatocytes, which is likely a result of a negative feedback loop for fatty acid synthesis, and IRS-2 protein levels were unaffected. FFA-induced insulin resistance has been reported in other insulin-sensitive cells, such as adipocytes (18) and skeletal muscle cells (26). These studies, together with the present results, suggest that FFA inhibits insulin signaling at the level of tyrosine phosphorylation of IRSs, regardless of cell type. Similar to the findings in 3T3-L1 adipocytes (18) and primary mouse hepatocytes and pancreatic β-cells (16), the activation of JNK, a known suppressor of the tyrosine phosphorylation of IRSs, was involved in FFA-induced tyrosine phosphorylation of IRS-2 in cultured H4IIEC3 hepatocytes. Because a JNK inhibitor, SP600125, largely restored palmitate-induced impairment of the insulin signaling pathway, JNK activation seems to play a major role in the development of palmitate-induced insulin resistance in H4IIEC3 hepatocytes. Our results support *in vivo* findings that JNK is activated in the liver of an animal model of obesity and diabetes in which FFA influx into the liver is elevated (9, 27). The overexpression of JNK in mouse liver resulted in hepatic insulin resistance at the level of IRS tyrosine phosphorylation, and the overexpression of a dominant negative mutant of JNK in the liver accelerated hepatic insulin signaling (17).

Given that JNK is activated by many types of cellular stresses (28), we next searched for a link between palmitate treatment and JNK activation in H4IIEC3 hepatocytes. ER stress was unlikely to mediate palmitate-induced insulin resistance in H4IIEC3 hepatocytes, because palmitate caused insulin resistance independent of ER stress, whereas tunicamycin caused ER stress without affecting insulin action. Instead, we found that palmitate-induced ROS generation mediated insulin resistance. ROS are one of many factors suggested to have a possible role in insulin resistance (29, 30). ROS include reactive products, such as superoxide anion, hydrogen peroxide, and

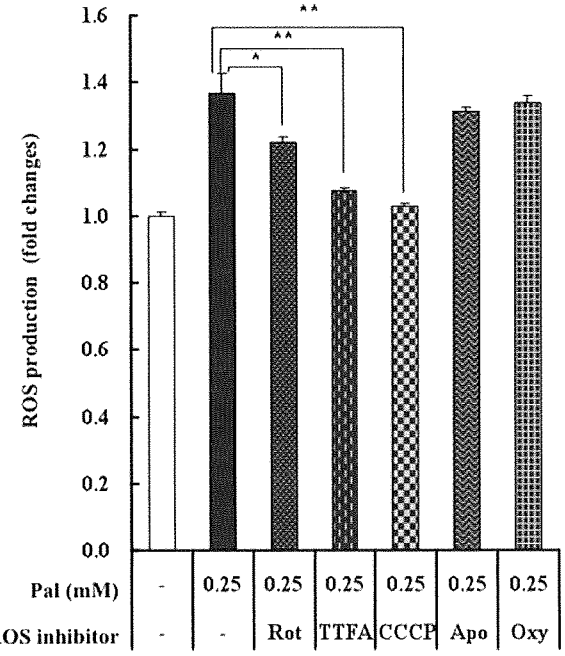

FIGURE 8. **Effects of ROS-producing pathway inhibitors on palmitate-induced ROS production in H4IIEC3 hepatocytes.** H4IIEC3 cells were incubated in the presence or absence of palmitate (*Pal*) and each ROS-producing pathway inhibitor for 8 h. Intracellular ROS production was quantified using the fluorescent probe H_2DCFDA. The values are expressed as mean -fold increase over control ± S.E. ($n = 4$). *, $p < 0.05$ *versus* palmitate treatment alone. **, $p < 0.01$ *versus* palmitate treatment alone. *Rot*, rotenone; *Apo*, apocynin; *Oxy*, oxypurinol; *TTFA*, thenoyltrifluoroacetone; *CCCP*, carbonyl cyanide *m*-chlorophenylhydrazone.

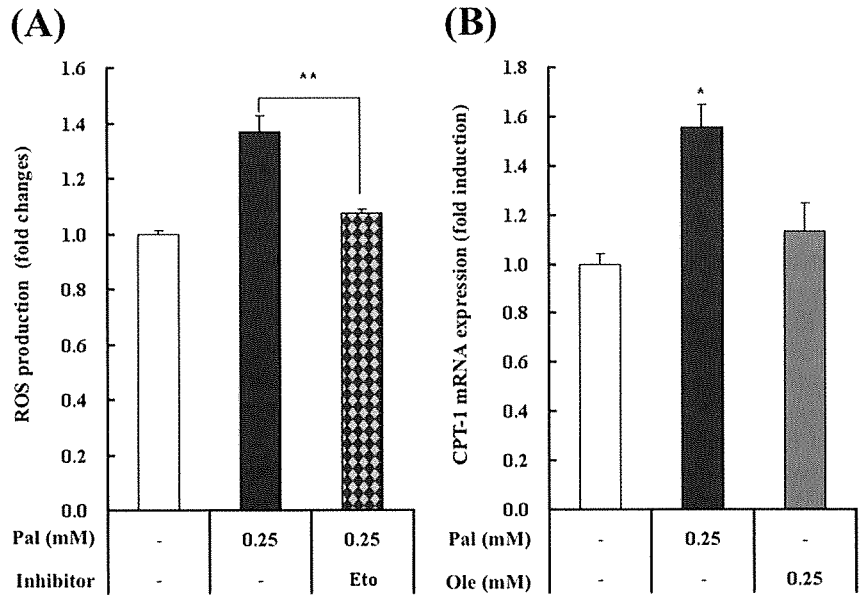

FIGURE 9. **Involvement of mitochondrial fatty acid oxidation in palmitate-induced ROS production.** *A*, H4IIEC3 cells were incubated in the presence or absence of palmitate (*Pal*) and the CPT-1 inhibitor etomoxir (*Eto*) for 8 h. Intracellular ROS production was quantified using the fluorescent probe H_2DCFDA. The values are expressed as mean -fold increase over control ± S.E. ($n = 4$). *B*, H4IIEC3 cells were incubated in the presence or absence of palmitate (*Pal*) or oleate (*Ole*) for 16 h. Total RNA was extracted and subjected to reverse transcription. Using the cDNA as a template, the amounts of CPT-1 mRNA were detected by real time PCR. The values were normalized to the level of 18 S ribosomal RNA and expressed as mean -fold increase over control ± S.E. ($n = 3$). *, $p < 0.05$ *versus* control. **, $p < 0.01$ *versus* palmitate treatment alone.

hydroxyl radical, which are formed as by-products of mitochondrial oxidative phosphorylation (OXPHOS). Thus, as a rule, increased mitochondrial OXPHOS flux leads to increased formation of ROS (31, 32). ROS can also be produced during β-oxidation of fatty acids, especially as a by-product of peroxisomal acyl-CoA oxidase activity (32). Additionally, ROS can be produced by dedicated enzymes, such as NADPH oxidase (33), present in phagocytic cells, where ROS are an important part of cellular defense mechanisms. Using specific inhibitors of subcellular ROS, we identified mitochondrial OXPHOS as an important source of palmitate-induced ROS generation in H4IIEC3 hepatocytes. FFAs supply mitochondrial OXPHOS with electrons through mitochondrial fatty acid β-oxidation. A final metabolite of fatty acids, acetyl-CoA, is metabolized in the trichloroacetic acid cycle. In the processes of fatty acid β-oxidation and the trichloroacetic acid cycle, NADH and $FADH_2$ are generated and could supply excessive electrons for OXPHOS.

NAC, a scavenger of ROS, dose-dependently restored glutathione in palmitate-treated cells (supplemental Fig. 5). However, glutathione restoration by NAC was unable to completely rescue palmitate-induced insulin resistance. Furthermore, the combination of NAC and α-tocopherol did not completely reverse JNK activation (supplemental Fig. 6, *A* and *B*) and only partly rescued palmitate-induced insulin resistance (supplemental Fig. 7, *A* and *B*). Therefore, other mechanisms may also be involved in insulin resistance caused by palmitate.

De novo ceramide synthesis is a potential pathway contributing to palmitate-induced JNK activation. Ceramide derived from saturated fatty acids has been reported to activate JNK and inhibit insulin-induced Akt phosphorylation in myocytes (34–36). In our investigation, palmitate increased the intracellular content of ceramide in H4IIEC3 hepatocytes (supplemental Fig. 8). Unfortunately, even at the maximum myriosin concentration, the intracellular accumulation of ceramide was not blocked by myriosin, a potent inhibitor of serine palmitoyltransferase at the first step in ceramide biosynthesis (supplemental Fig. 8). Furthermore, ceramide accumulation was not blocked when myriosin was used in combination with fumonisin B1, an inhibitor of ceramide synthase (data not shown). Therefore, we cannot rule out the possibility that intracellular ceramide contributes to palmitate-induced insulin resistance in H4IIEC3 hepatocytes. Further studies are required to assess the role of the

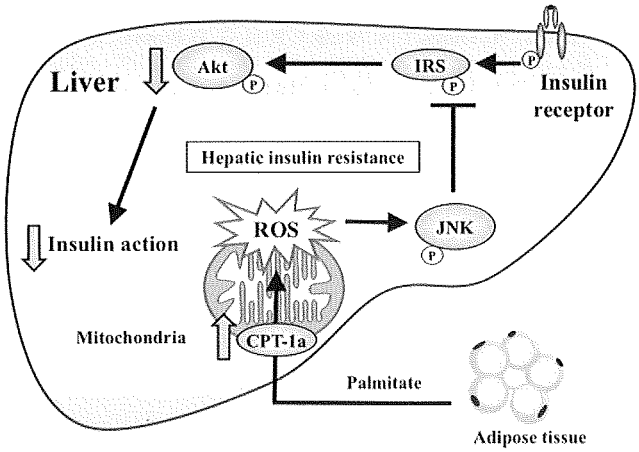

FIGURE 10. **Proposed model for palmitate-induced hepatic insulin resistance.**

ceramide pathway in palmitate-induced insulin resistance in hepatocytes.

In the present study, etomoxir, an inhibitor of CPT-1, decreased palmitate-induced intracellular ROS production. Additionally, palmitate, but not oleate, significantly increased the expression of the *CPT-1a* gene, which may account for the observed differences in insulin action between palmitate and oleate.

Recently, it was reported that fatty acid composition may be a determinant in insulin sensitivity (37, 38). In this regard, we investigated the effect of oleate on insulin signaling in palmitate-treated hepatocytes. Surprisingly, oleate dose-dependently reversed palmitate-induced ROS generation and JNK phosphorylation and rescued palmitate-induced phosphorylation of Akt.[3] Further investigations aimed at elucidating the molecular basis underlying the differential roles and interactions of FFAs are required.

In conclusion, this study identified mitochondrial ROS generation as a critical factor in palmitate-induced hepatic insulin resistance. Palmitate may induce CPT-1 expression, accelerate metabolism, supply excess electrons for mitochondrial OXPHOS, and generate ROS. ROS then desensitize the insulin signaling pathway by activating JNK, impairing tyrosine phosphorylation of IRS-2, and causing hepatic insulin resistance (Fig. 10). The results suggest that an initial event in high fat/sucrose diet-induced or obesity-induced insulin resistance in the liver is mitochondrial ROS generation, which could potentially be a therapeutic target. In addition to previously suggested JNK inhibitors or antioxidants, mitochondrial uncouplers, such as cyanide *m*-chlorophenylhydrazone, may provide a candidate therapeutic strategy for this pathway by preventing ROS generation.

Acknowledgments—We thank Drs. Isao Usui and Hajime Ishihara and Prof. Toshiyasu Sasaoka (Toyama University) for supplying technical expertise on Western blot analysis of phosphoproteins.

[3] H. Takayama and T. Takamura, unpublished data.

REFERENCES

1. Saltiel, A. R., and Kahn, C. R. (2001) *Nature* **414,** 799–806
2. Ota, T., Takamura, T., Kurita, S., Matsuzawa, N., Kita, Y., Uno, M., Akahori, H., Misu, H., Sakurai, M., Zen, Y., Nakanuma, Y., and Kaneko, S. (2007) *Gastroenterology* **132,** 282–293
3. Matsuzawa, N., Takamura, T., Kurita, S., Misu, H., Ota, T., Ando, H., Yokoyama, M., Honda, M., Zen, Y., Nakanuma, Y., Miyamoto, K., and Kaneko, S. (2007) *Hepatology* **46,** 1392–1403
4. Sakurai, M., Takamura, T., Ota, T., Ando, H., Akahori, H., Kaji, K., Sasaki, M., Nakanuma, Y., Miura, K., and Kaneko, S. (2007) *J. Gastroenterol.* **42,** 312–317
5. Boden, G. (1997) *Diabetes* **46,** 3–10
6. Ide, T., Shimano, H., Yahagi, N., Matsuzaka, T., Nakakuki, M., Yamamoto, T., Nakagawa, Y., Takahashi, A., Suzuki, H., Sone, H., Toyoshima, H., Fukamizu, A., and Yamada, N. (2004) *Nat. Cell Biol.* **6,** 351–357
7. Hirosumi, J., Tuncman, G., Chang, L., Gorgun, C. Z., Uysal, K. T., Maeda, K., Karin, M., and Hotamisligil, G. S. (2002) *Nature* **420,** 333–336
8. Boden, G., She, P., Mozzoli, M., Cheung, P., Gumireddy, K., Reddy, P., Xiang, X., Luo, Z., and Ruderman, N. (2005) *Diabetes* **54,** 3458–3465
9. Ozcan, U., Cao, Q., Yilmaz, E., Lee, A. H., Iwakoshi, N. N., Ozdelen, E., Tuncman, G., Gorgun, C., Glimcher, L. H., and Hotamisligil, G. S. (2004) *Science* **306,** 457–461
10. Kim, J. K., Fillmore, J. J., Chen, Y., Yu, C., Moore, I. K., Pypaert, M., Lutz, E. P., Kako, Y., Velez-Carrasco, W., Goldberg, I. J., Breslow, J. L., and Shulman, G. I. (2001) *Proc. Natl. Acad. Sci. U. S. A.* **98,** 7522–7527
11. Turinsky, J., O'Sullivan, D. M., and Bayly, B. P. (1990) *J. Biol. Chem.* **265,** 16880–16885
12. Du, K., Herzig, S., Kulkarni, R. N., and Montminy, M. (2003) *Science* **300,** 1574–1577
13. Nishikawa, T., Edelstein, D., Du, X. L., Yamagishi, S., Matsumura, T., Kaneda, Y., Yorek, M. A., Beebe, D., Oates, P. J., Hammes, H. P., Giardino, I., and Brownlee, M. (2000) *Nature* **404,** 787–790
14. Matsuzawa-Nagata, N., Takamura, T., Ando, H., Nakamura, S., Kurita, S., Misu, H., Ota, T., Yokoyama, M., Honda, M., Miyamoto, K., and Kaneko, S. (2008) *Metabolism* **57,** 1071–1077
15. Aguirre, V., Uchida, T., Yenush, L., Davis, R., and White, M. F. (2000) *J. Biol. Chem.* **275,** 9047–9054
16. Solinas, G., Naugler, W., Galimi, F., Lee, M. S., and Karin, M. (2006) *Proc. Natl. Acad. Sci. U. S. A.* **103,** 16454–16459
17. Nakatani, Y., Kaneto, H., Kawamori, D., Hatazaki, M., Miyatsuka, T., Matsuoka, T. A., Kajimoto, Y., Matsuhisa, M., Yamasaki, Y., and Hori, M. (2004) *J. Biol. Chem.* **279,** 45803–45809
18. Nguyen, M. T., Satoh, H., Favelyukis, S., Babendure, J. L., Imamura, T., Sbodio, J. I., Zalevsky, J., Dahiyat, B. I., Chi, N. W., and Olefsky, J. M. (2005) *J. Biol. Chem.* **280,** 35361–35371
19. Bennett, B. L., Sasaki, D. T., Murray, B. W., O'Leary, E. C., Sakata, S. T., Xu, W., Leisten, J. C., Motiwala, A., Pierce, S., Satoh, Y., Bhagwat, S. S., Manning, A. M., and Anderson, D. W. (2001) *Proc. Natl. Acad. Sci. U. S. A.* **98,** 13681–13686
20. Karaskov, E., Scott, C., Zhang, L., Teodoro, T., Ravazzola, M., and Volchuk, A. (2006) *Endocrinology* **147,** 3398–3407
21. Harding, H. P., Calfon, M., Urano, F., Novoa, I., and Ron, D. (2002) *Annu. Rev. Cell Dev. Biol.* **18,** 575–599
22. Kaneto, H., Kawamori, D., Nakatani, Y., Gorogawa, S., and Matsuoka, T. A. (2004) *Drug News Perspect.* **17,** 447–453
23. Furukawa, S., Fujita, T., Shimabukuro, M., Iwaki, M., Yamada, Y., Nakajima, Y., Nakayama, O., Makishima, M., Matsuda, M., and Shimomura, I. (2004) *J. Clin. Invest.* **114,** 1752–1761
24. Carlsson, C., Borg, L. A., and Welsh, N. (1999) *Endocrinology* **140,** 3422–3428
25. Miller, T. A., LeBrasseur, N. K., Cote, G. M., Trucillo, M. P., Pimentel, D. R., Ido, Y., Ruderman, N. B., and Sawyer, D. B. (2005) *Biochem. Biophys. Res. Commun.* **336,** 309–315
26. Chavez, J. A., and Summers, S. A. (2003) *Arch. Biochem. Biophys.* **419,** 101–109
27. Nakatani, Y., Kaneto, H., Kawamori, D., Yoshiuchi, K., Hatazaki, M., Mat-

suoka, T. A., Ozawa, K., Ogawa, S., Hori, M., Yamasaki, Y., and Matsuhisa, M. (2005) *J. Biol. Chem.* **280,** 847–851
28. Davis, R. J. (2000) *Cell* **103,** 239–252
29. Evans, J. L., Goldfine, I. D., Maddux, B. A., and Grodsky, G. M. (2002) *Endocr. Rev.* **23,** 599–622
30. Houstis, N., Rosen, E. D., and Lander, E. S. (2006) *Nature* **440,** 944–948
31. Brownlee, M. (2001) *Nature* **414,** 813–820
32. Osmundsen, H., Bremer, J., and Pedersen, J. I. (1991) *Biochim. Biophys. Acta* **1085,** 141–158
33. De Minicis, S., Bataller, R., and Brenner, D. A. (2006) *Gastroenterology* **131,** 272–275
34. Chavez, J. A., Knotts, T. A., Wang, L. P., Li, G., Dobrowsky, R. T., Florant, G. L., and Summers, S. A. (2003) *J. Biol. Chem.* **278,** 10297–10303
35. Powell, D. J., Turban, S., Gray, A., Hajduch, E., and Hundal, H. S. (2004) *Biochem. J.* **382,** 619–629
36. Schmitz-Peiffer, C., Craig, D. L., and Biden, T. J. (1999) *J. Biol. Chem.* **274,** 24202–24210
37. Bruce, C. R., and Febbraio, M. A. (2007) *Nat. Med.* **13,** 1137–1138
38. Cao, H., Gerhold, K., Mayers, J. R., Wiest, M. M., Watkins, S. M., and Hotamisligil, G. S. (2008) *Cell* **134,** 933–944

DIABETICMedicine

DOI: 10.1111/j.1464-5491.2009.02773.x

Original Article: Pathophysiology

J-shaped relationship between waist circumference and subsequent risk for Type 2 diabetes: an 8-year follow-up of relatively lean Japanese individuals

M. Sakurai, K. Miura*, T. Takamura†, M. Ishizaki‡, Y. Morikawa, K. Nakamura, K. Yoshita§, T. Kido¶, Y. Naruse**, S. Kaneko† and H. Nakagawa

Department of Epidemiology and Public Health, Kanazawa Medical University, Ishikawa, Japan, *Department of Health Science, Shiga University of Medical Science, Otsu, Japan, †Department of Disease Control and Homeostasis, Kanazawa University Graduate School of Medical Science, Kanazawa, Japan, ‡Department of Social and Environmental Medicine, Kanazawa Medical University, Ishikawa, Japan, §Division of Health and Nutrition Monitoring, National Institute of Health and Nutrition, Tokyo, Japan, ¶Department of Community Nursing, Kanazawa University School of Health Sciences, Kanazawa, Japan and **Department of Community and Geriatric Nursing, Toyama University, Toyama, Japan

Accepted 22 May 2009

Abstract

Aims This study investigated the relationship between waist circumference and the subsequent incidence of Type 2 diabetes and the association with insulin resistance and pancreatic B-cell function in relatively lean Japanese individuals.

Methods The study participants were 3992 employees (2533 men and 1459 women, aged 35–55 years) of a metal-products factory in Japan. The incidence of diabetes was determined in annual medical examinations during an 8-year follow-up. We calculated age- and sex-adjusted hazard ratios (HRs) according to the sex-specific quintile of waist circumference at baseline. Differences in baseline insulin resistance [homeostatis model assessment (HOMA)-IR] and pancreatic B-cell function (HOMA-B) were compared between participants who developed diabetes and those who did not.

Results During the follow-up, 218 participants developed diabetes. Age- and sex-adjusted HRs across the quintiles of waist circumference were 1.78, 1.00 (reference), 1.59, 3.11 and 3.30, respectively (P for trend, < 0.0001). The HR for the lowest quintile was significantly higher than that for the second quintile. Among participants with waist circumference of the lowest quintile, HOMA-B was lower in those who developed diabetes than in those who did not [33.1 (24.1–45.0) vs. 54.3 (37.9–74.6) median (interquartile range), $P < 0.0001$], but HOMA-IR did not differ between these groups.

Conclusions There was a J-shaped relationship between waist circumference and subsequent risk for Type 2 diabetes in relatively lean Japanese individuals; lower pancreatic B-cell function may also increase the risk of diabetes in very lean Japanese people.

Diabet. Med. 26, 753–759 (2009)

Keywords Incidence, insulin resistance, insulin secretion, Type 2 diabetes, waist circumference

Abbreviations BMI, body mass index; HbA_{1c}, glycated haemoglobin; HDL, high-density lipoprotein; HOMA-B, homeostasis model assessment of pancreatic B-cell function; HOMA-IR, homeostasis model assessment of insulin resistance; HR, hazard ratio; OGTT, oral glucose tolerance test

Introduction

Obesity increases the risk for Type 2 diabetes [1–7], with previous reports indicating a linear association between the degree of obesity and the incidence of Type 2 diabetes in Western populations [1–5]. Although the prevalence of obesity is much lower in Asian countries than in Western countries, the prevalence of Type 2 diabetes has been reported to be similar [8], suggesting that the association between obesity and diabetes may be different in Asian countries compared with Western countries.

One possible reason for the high frequency of Type 2 diabetes in Asians is the presence of prominent abdominal fat in Asians compared with Caucasians with a similar body mass index (BMI)

Correspondence to: Masaru Sakurai, MD, PhD, Department of Epidemiology and Public Health, Kanazawa Medical University, 1-1 Daigaku, Uchinada, Ishikawa, 920-0293, Japan. E-mail: m-sakura@kanazawa-med.ac.jp

[9,10]; however, few studies have analysed the association between waist circumference and diabetic risk in Asians [11]. Waist circumference might be a useful predictor for diabetes in Asians with high abdominal fat.

In addition to obesity, impairment of early phase insulin secretion and low pancreatic B-cell mass may play important roles in the development of Type 2 diabetes in lean Asians [12–15]. Decreased B-cell function can cause hyperglycaemia prior to the onset of obesity. It is possible that not only obese people with insulin resistance but also lean people with lower B-cell function are at high risk for developing Type 2 diabetes. Recently, a J-curve association between BMI and the incidence of diabetes was reported in older Japanese adults [16]. This report suggested that older Japanese people with low BMI would also be at higher risk for developing diabetes. However, there have been few prospective studies investigating the relationship of waist circumference to future development of diabetes in lean Asian people which have also assessed B-cell function and insulin resistance.

In this large, 8-year prospective study of relatively lean Japanese men and women, we investigated the relationship between anthropometric indices (BMI and waist circumference) and the subsequent risk for developing Type 2 diabetes. The objectives of this study were: (i) to investigate whether waist circumference is associated with the future risk of diabetes; (ii) to determine whether the relationship is linear or J-shaped; (iii) to investigate how this relationship is influenced by insulin resistance and B-cell function.

Research design and methods

The participants were employees of a factory that produces zip fasteners and aluminum sashes in Toyama Prefecture, Japan. Detailed information about the study population has been described [17–19]. The Industrial Safety and Health Law in Japan requires employers to conduct annual health examinations of all employees. A survey of the incidence of diabetes mellitus was performed during the annual medical examinations between 1996 and 2004. At the baseline examination in 1996, 4274 (90%) of 4757 employees aged 35–55 years received health examinations. Of these 4274 potential participants, 282 (6.6%) were excluded: 199 had pre-existing diabetes or had high fasting plasma glucose (≥ 7.0 mmol/l) at the time of the baseline examination, 16 had missing data in baseline anthropometric indices and 67 did not participate in consecutive follow-up annual health examinations. The final study population consisted of 3992 employees (2533 men and 1459 women).

The baseline health examination included a medical history, physical examination, anthropometric measurements (waist circumference and BMI) and the determination of fasting plasma glucose, fasting insulin, glycated haemoglobin (HbA_{1c}) and serum lipid levels. Height was measured, without shoes, to the nearest 0.1 cm using a stadiometer. Weight was measured, with participants wearing only light clothing and no shoes, to the nearest 0.1 kg using a standard scale. BMI was calculated as weight/height^2 (kg/m^2). Waist circumference was determined to the nearest 0.5 cm by measuring from a point above the iliac crest and below the lowest rib margin, during minimal respiration in a standing position. Blood pressure was measured once with a mercury sphygmomanometer after the subjects had rested for 5 min in a seated position. Trained staff took all of the measurements.

Plasma glucose levels were measured enzymatically (Abbott glucose UV test; Abbott Laboratories, Chicago, IL, USA) and plasma insulin levels were determined by radioimmunoassay (Shionogi Co., Tokyo, Japan). HbA_{1c} was measured by high-velocity liquid chromatography using a fully automated analyser (Kyoto Daiichi Kagaku, Kyoto, Japan). Total cholesterol and triglycerides were measured by enzyme assay. High-density lipoprotein (HDL) cholesterol was measured by direct method. Insulin resistance was calculated by the homeostasis model assessment (HOMA) method [20], using the following;

$$\text{HOMA-IR} = \text{fasting insulin}\ (\mu\text{U/ml}) \times \text{fasting plasma glucose}\ (\text{mmol/l})/22.5$$

The HOMA of pancreatic B-cell function (HOMA-B) [20] was calculated using the following;

$$\text{HOMA-B} = 20 \times \text{fasting insulin}\ (\mu\text{U/ml})/[\text{fasting plasma glucose}\ (\text{mmol/l}) - 3.5]$$

Participants with $HbA_{1c} > 6.0\%$ underwent a 75-g oral glucose tolerance test (OGTT). According to the definitions of the American Diabetes Association [21] and the Japanese Diabetes Society [22], the diagnosis of diabetes is confirmed by at least one of the following observations: (i) fasting plasma glucose concentration ≥ 7.0 mmol/l; (ii) 2-h glucose level ≥ 11.1 mmol/l in a 75-g OGTT; or (iii) treatment with insulin or oral glucose-lowering agents.

A questionnaire was used to identify lifestyle behaviours such as alcohol consumption, smoking and regular exercise. Participants were classified as either non-drinkers or active drinkers. Active drinkers were further divided into occasional (less than 5 days/week), light (more than 5 days/week and average amounts less than 40 g alcohol/day for men and 20 g/day for women) or moderate/heavy (more than 5 days/week and average amounts of more than 40 g alcohol/day for men and 20 g/day for women) drinkers. Data were also collected concerning smoking habits (never, ex-smoker or current smoker) and frequency of exercise (none, weak, moderate or strong). Exercise was defined as the participation in any physical activity such as jogging, cycling, swimming or tennis that was performed long enough to cause sweating. A self-administered questionnaire was also used to collect information about a medical history of hypertension, dyslipidaemia, diabetes and the use of glucose-lowering medication. High blood pressure and dyslipidaemia were defined by the Japanese criteria of the

